Towards High Fidelity Aeroacoustics Interior Noise Prediction

Mauricio Massarotti[1], Simon Martin[2], Joseph Venor[2]

[1]Whole-Vehicle Acoustics, Bentley Motors
Crewe, England, United Kingdom
mauricio.ramacciato.massarotti@bentley.co.uk

[2]Vibro-Acoustic Technical Consultancy, ESI Group
Birmingham, England, United Kingdom
simon.martin@esi-group.com, joseph.venor@esi-group.com

Abstract: Acoustic refinement is of paramount importance in luxury vehicles, and so therefore is the search for state-of-the-art engineering methods to aid development. This work concerns the application of unsteady compressible CFD and whole-vehicle Aero-Vibroacoustic models to predict interior Aeroacoustic noise from 250 to 5kHz at high cruising speeds. The primary objective of this project is to improve the correlation between fast Greenhouse interior noise predictions to actual measurements made in an Aeroacoustic Wind Tunnel by using the CFD outputs as inputs to whole-vehicle Vibroacoustic SEA models. More accurate base Aeroacoustic predictions lead to more accurate early Project status, a more realistic experience in the NVH Simulator and ultimately robust decisions taken on the overall attribute balancing. Previous studies have demonstrated an interior noise correlation offset of 2 dB across the entire frequency range of interest at an overshot computational cost. Improvements made in fluid discretization, transient time scales, SEA model content and linear panel characterization enabled equally or more accurate results at significantly lower footprint.

1 Introduction

Aeroacoustics is one of the primary attributes in luxury vehicles. Within a rapidly developing technology landscape and evolving marketplace, engineers need reliable tools to predict the whole-vehicle Aeroacoustic performance of new products early in the development process. Total Aeroacoustic performance comprises of multiple components such as residual aspiration, discrete phenomena (e.g. aeolian tones, cavity resonance and acoustic feedback), open aperture buffeting and exterior airflow-induced broadband noise, typically known as "Greenhouse Wind Noise". The latter is complex in itself as it encompasses sources of different nature distributed on the Upper Body and Underbody panels, which are transmitted through multiple paths including glazing panels, sealing systems and acoustic lining. In steady-state, the characteristic frequency band is extremely large, audible in the cabin from 250 to 5kHz and above at high cruising speeds. As a rough estimate, sound at frequencies lower than 500-600Hz are typically dominated by sources on the Underbody, and at higher frequency from sources on the Upper Body, as well as their transmission paths. A ride in the Wind Tunnel makes it very clear.

Typically, the first opportunity the Aeroacoustics engineers have to validate the performance of such is by measuring the first off-tooling prototype builds in a Full-Scale Aeroacoustic Wind Tunnel. Common to many OEMs, the vehicles are measured in "masked" condition enabling the separation (root causing analysis) of discrete phenomena, localized aspiration and general source ranking. During Concept phases, Full-Size Clay models built with an acoustic cavity are limited in that purpose as transfer paths are not representative. Numerically, the fast approach, computationally less expensive, is to compute the total pressure field impinging on the glazing panels, either via Hybrid- or Direct Noise Computation, transmit and propagate the noise to the Passenger compartment via multiple Aero-Vibroacoustic formulations based on SEA, FEM and BEM, each with its advantages and limitations [1]. Such approach suffice should one be interested in statusing the Aeroacoustic performance of the vehicle's exterior surface alone, in regards of dipole and quadrupole sound generation mechanisms, as well as assessing the specification of the glazing panels in itself, as unquestionably, some of the glazing panels are the primary transfer path of high frequency broadband Aeroacoustic noise in masked condition.

In luxury vehicles, however, glazing specifications are typically of high specification acoustic attributes, causing other transmission paths to contribute significantly to the whole-vehicle experience. In that sense, it is extremely valid to status (as a key Concept gateway) the predicted whole-vehicle Aeroacoustic performance including Upper Body, Underbody and all the relevant insulation and damping aspects of the Project in scope. To that extent, the reuse of whole-vehicle Vibro-Acoustic SEA models applied to other NVH attributes such as Airborne Road Noise becomes cost attractive.

The method was initially validated on Bentley's third generation luxury sports coupé Continental GT [2]. The final interior 1/3 Octave noise spectra offset between model and test is in the order of 1 to 3 dB across the entire frequency span, proving excellent value. The whole-vehicle SEA model also enables a more complete source ranking including Upper Body and Underbody transfer paths not modelled in typical Greenhouse models. Previous work demonstrated that the transmission of high frequency noise through the A-Pillar body panels and trim is significant in amplitude thus relevant to the front occupants. Those findings are based on a single stationary flow condition at null incidence angle. Once the pressure gradients are higher in non-zero yaw and unsteady flows, the importance of evaluating the A-Pillar transfer path is of critical importance. The CFD computational effort required by the proven method, however, is knowingly excessive as a means of guaranteeing all vorticity scales and target frequencies are captured. As suggested, the present work intends to re-validate the model in a SUV Bodystyle adopting less aggressive grid and time transient scales, whilst maintaining the output quality.

2 Fluid Solution

The numerical fluid solution is divided in two different domains: the Upper Body and the Underbody. Each domain is resolved separately at specific grid and time transient scales determined by the target frequencies. Although possible, the solution of the entire domain in a single submission would result in significantly higher computational effort. It is possible to run the simulations separately since the pressure loads are exported independently and coupled to a second Aero-Vibroacoustic solver.

The Upper Body solution requires finer fluid cells iterated at faster pace to account for the smallest vortices and highest frequencies, whilst the Underbody runs on a coarser grid and larger timestep for a longer interval. Figure 1 shows the finest and second finest Volumetric elements (Voxels) in both domains. The total pressure field (hydrodynamic plus acoustic) of both cases is resolved using Lattice-Boltzmann lagrangian formulation (LBM), Very Large Eddy Simulation (VLES) approach and re-normalized (RNG) k-ε Turbulence Model. The Boundary Layer flow over the vehicle surfaces is modelled rather than resolved by an extension of the standard law-of-the-wall formulation, which is acceptable in low Mach applications once source terms within the Turbulent Boundary Layer (TBL) can be neglected. The flow solution is inherently unsteady and compressible, and the near-field sound pressure is computed directly due to low numerical dissipation and dispersion properties. SIMULIA PowerFLOW® is the solver of choice for the fluid computation [3,4]. Characteristic flow properties are described in Table A. Surface and fluid discretization, time transient settings and computational efforts are summarized in Table B. Compared to previous work [2], significant computational savings achieved in both Upper Body and Underbody solutions are attributed to the reduction of the finest Voxel count and number of timesteps run for a shorter physical time.

VR = 1mm VR = 0.5mm

VR = 2mm VR = 1mm

Figure 1: Finest and second finest Voxel resolution on the Upper Body and Underbody fluid domains (VR = Variable Resolution)

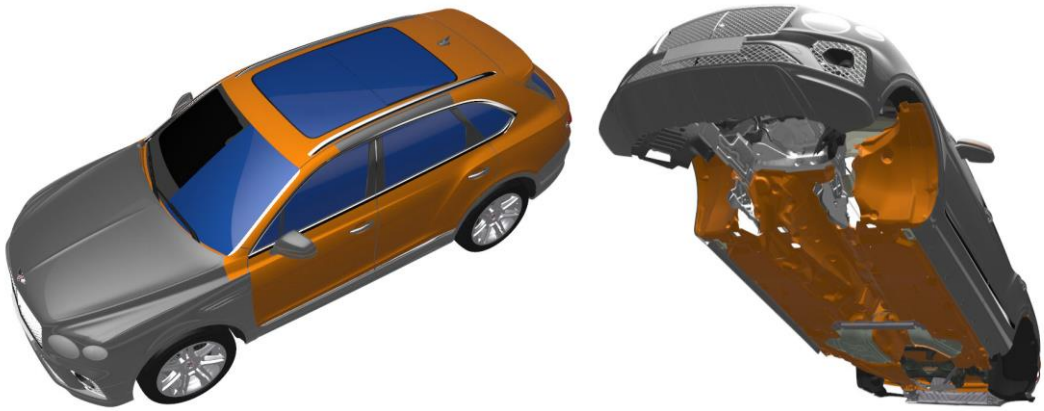

Figure 2: Pressure load measurement panels

Table A: Characteristic flow properties

Wheels and Floor	Stationary
Flow Velocity, km/h (m/s)	140 (38.89)
Incident Yaw Angle, °	0
Flow Mach Number	0.11
Simulation Mach Number	0.11
Reynolds Number	2.61e+06
Incoming Turbulence Intensity	1%

Table B: Discretization, transient settings and computational effort

Parameter	Upper Body	Underbody
Body Representation	Symmetry Model	Full Model
Frequency of Interest, kHz	0.5 – 5	0.25 – 1
Fine-Equivalent Surfel Count	24,173,956	49,070,870
Minimum Wall Cell Size, mm	0.5	1
Fine-Equivalent Voxel Count	185,423,888	253,104,575
Physical Time, s (past settling)	0.6 (past settling)	2 (incl. settling)
Timestep, s	8.34e-7	2.10e-6
Number of Time Steps	719,390	713,332
Measurement Interval, s	Last 0.5	Last 1.5
Number of Processor Cores	431	479
Total Clock Time, h	75.75	116.6
Total CPU Time, h	32,648	55,851

Once solution is completed, the pressure excitation over 47 different panels and segments of panels are output in the form of standard transient surface measurement CGNS files (CFD General Notation System), totalling 87Gb of data once compressed. The surface mesh coordinates are also converted in uniform grids of 2 to 8mm depending on the panel. The CGNS files contain the pressure time history recorded at pre-defined sampling, at all mesh coordinates of each panel. Upper Body and Underbody measurement panels are illustrated in blue (glazing) and orange in Figure 2.

3 Aero-Vibroacoustic Modelling

3.1 Statistical Energy Analysis

Statistical Energy Analysis (SEA) is an established methodology to perform interior noise and vibration predictions to support both acoustic and structural package development. In the automotive industry, SEA is widely used for the interior airborne noise prediction from sources from 250Hz and includes the ability to model the energy contribution through various transmission paths as in an actual vehicle by the use of reference acoustic sources [5]. For this project, the SEA software VAOne® is used.

3.2 Model Description

The present SEA model was originally built for road and powertrain noise development. The model was defined to provide the best understanding of the energy flow around and within the vehicle, enabling a large variety of analyses. The exterior sound field was comprised of near and mid field cavities defined and connected to ensure the correct exterior acoustic power input at all locations. The mid field cavities were also connected to a semi-infinite fluid (Figure 3) to represent an unbounded exterior acoustic space. The Coupling Loss Factors (CLF) between SEA subsystems were analytically derived and calculated automatically by the software. The Damping Loss Factors (DLF) of subsystems are defined based on test data, and the SEA model considers both resonant and non-resonant propagation transfer paths, with the total contributions and energy flows being the sum of both. Previous validation cases have shown that in a typical vehicle cabin, the direct field contribution is negligible compared to the reverberant field response at the frequencies mostly contributing to the interior noise (above 250Hz, where the acoustic wavelength is less than a meter and the distance between side glasses and occupant ears is substantially less than a quarter wavelength).

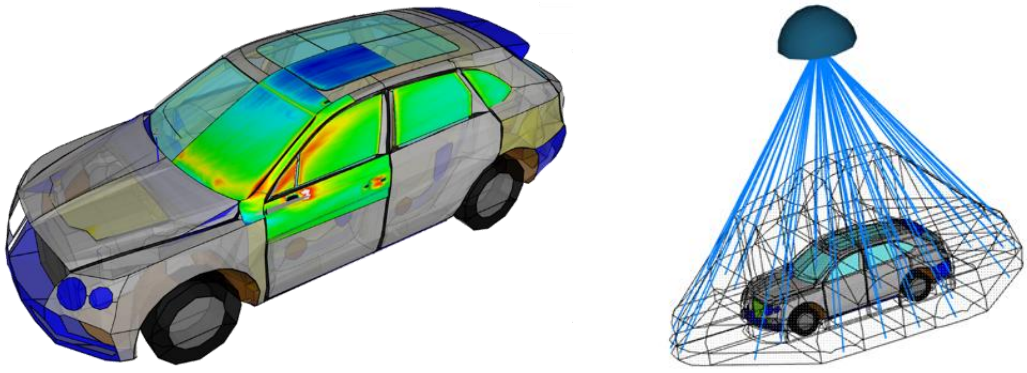

Figure 3: Visual representation of the whole-vehicle SEA model (left) & its exterior sound field (right)

3.3 Aero-Vibroacoustic (AVA) Data Import

To extract the excitations to be applied on the SEA model, the surface measurements from compressible CFD were post-processed by converting the total fluctuating surface pressure into a combination of a Turbulent Boundary Layer (TBL) representing the convective component, and a Diffuse Acoustic Field (DAF) representing the acoustic component. A visual overview of the end-to-end process from transient surface pressures to excitation loads applied on the SEA model is shown in Figure 4.

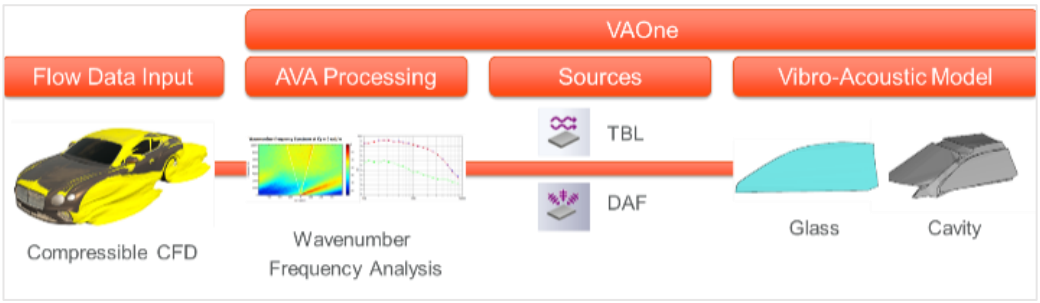

Figure 4: Data conversion process from CFD to SEA Vibroacoustic model

Initially, the fluctuating surface pressure results obtained from the CFD are processed into a two dimensional Wavenumber Frequency Spectrum (WFS). This wavenumber analysis allows movement from the time domain to the frequency domain, and from a two-dimensional physical space to a two-dimensional wavenumber space in the flow direction (k_x) and cross-flow direction (k_y). Although the glasses are slightly curved, a projection to a flat panel for the wavenumber transform is acceptable given the small scale of the acoustic wavelength for the frequencies of interest relative to the radius of curvature. Once the wavenumber frequency spectrum is obtained, it is possible to separate and extract the convective and acoustic components.

Equation (1) describes the Wavenumber Frequency Spectrum $S_{pp}(k, f)$, as a two-dimensional spatial Fourier Transform of the Pressure Correlation Spectrum $R_{pp}(r, f)$. The Pressure Correlation Spectrum is an average pressure at a given location, conjugated with a pressure at another location. $F[*]$ is the Fourier transform operator.

Equation (2) describes the power of the signal associated with the wavelengths inside the acoustic circle. The Wavenumber Frequency Spectrum $S_{pp}(k, f_i)$ is integrated from 0 to the acoustic wavenumber a_{k0}. Equation (3) is similar to Equation (2) but calculates the power of the signal associated with all other wavelengths outside of the acoustic circle, i.e. the convective component.

Along the k_x axis of a Wavenumber Frequency Spectrum (Figure 5a), the convective component is identified as travelling downstream with an inclination equal to the flow speed. The acoustic cone, with an inclination equal to the speed of sound, is integrated to obtain the acoustic component.

The wavenumber analysis acoustic cone can be seen to be tilted slightly to the left of the theoretical acoustic cone (white lines in Figure 5a). This is the result of Doppler shift whereby the flow velocity affects the relative velocity of sound. The observation shows the convective component is in the flow direction only (positive k_x) centred around the convective wavenumber whereas the acoustic cone shows the acoustics having an upstream as well as a downstream direction with energy concentrated near the acoustic wavenumber in both upstream and downstream directions.

$$S_{pp}(k,f) = F\,[R_{pp}(r,f)] \tag{1}$$

$$P_{\mathrm{ac}}(f_i) = \int_0^{|a_{k0}|} S_{pp}(k,f_i)dk \tag{2}$$

$$P_{\mathrm{co}}(f_i) = \int_{|k|>a_{k0}}^{|k_{\max}|} S_{pp}(k,f_i)dk \tag{3}$$

Where,

S_{pp}	=	Wavenumber Frequency Spectrum
k	=	Wavenumber
f	=	Frequency
F	=	Fourier Transform Operator
R_{pp}	=	Pressure Cross-correlation Spectrum
r	=	Node position
P_{ac}	=	Acoustic Autopower Spectrum
f_i	=	Frequency increment
a_{k0}	=	Acoustic wavenumber
P_{co}	=	Convective Power
k_{max}	=	Maximum Wavenumber of interest

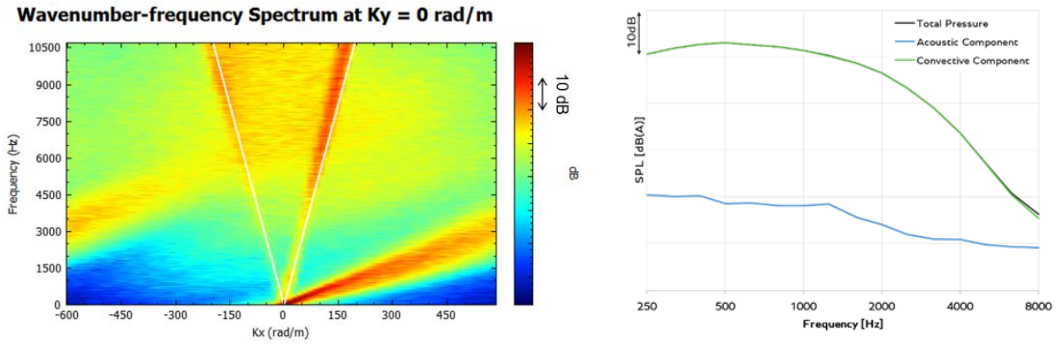

(a) (b)

Figure 5: (a) Wavenumber Frequency Spectrum on side glazing panel (k_x direction); (b) Resulting 1/3 Octave acoustic & convective components.

The result of a wavenumber separation into acoustic and convective components can be seen in Figure 5b. The convective component is significantly greater in magnitude than the acoustic, but the acoustic component must not be omitted due to the broad frequency range of interest (250-8kHz). The stronger coupling between the acoustic component to interior noise due to resonant and non-resonant transmission of the energy, means that the acoustic component dominates over a substantial part of the frequency range, even though the excitation level is significantly lower [1].

Ultimately, the convective component is applied as a Turbulent Boundary Layer excitation to the SEA model on the vehicle panels. Where the spectrum is specified by that extracted from the wavenumber analysis, and the appropriate area modifier applied dependent upon the examination of specific turbulent zones. The acoustic component is applied as a Diffuse Acoustic Field, at the level of the acoustic component extracted from the wavenumber analysis, and applied to a face of the near field external cavities.

4 Validation Experiment

Previous validation experiments conducted in a sports coupé [2] proves the potential of achieving a correlation offset of 1 to 3dB in all 1/3 Octave bands from 250 to 5kHz. In the present project, interior noise correlation measurements replicating the CAE setup to its best are taken in the Full-Scale Aeroacoustic Wind Tunnel of FKFS© (Figure 6). Sealing shutlines and part matching interfaces are taped to prevent localized flow & noise phenomena not modelled in CFD, as well as residual aspiration. Binaural and multiple free-field recordings are taken in the driver's seating compartment. Given the nature of SEA, the energy of inner and outer ears was averaged for each head location in order to provide comparable results. The measurements are taken for 30s and data is sampled at 48kHz.

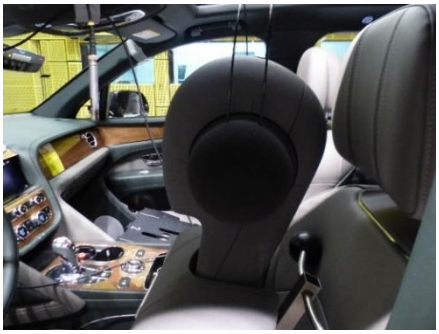

Figure 6: Validation test setup

4.1 Whole-Vehicle Interior Noise

Modelled and tested interior noise at the front head position are shown in Figure 7, along with the zonal contribution from Glazing, Body and Underbody Panels, bounded by the minima and maxima of each part group. “AAWT” stands for Aeroacoustic Wind Tunnel testing data. Below 1kHz, the methods are in good agreement with an offset from 1 to 3 dB. Above 1kHz, excellent agreement is met with a difference in decimal order in most 1/3 Octave bands. In the front driver location, windscreen and side glass panels are the top contributors above 500Hz, and body cavities such as A-Pillar and doors dominate over roof and rear glazing. Those findings indicate the modelling of body and trim components is relevant to predict the interior noise with due accuracy, in particular for this vehicle where glazing paths are highly damped for high frequency noise. Below 500Hz, noise from Underbody panels such as under trays and wheel arches dominate as expected (Figure 8).

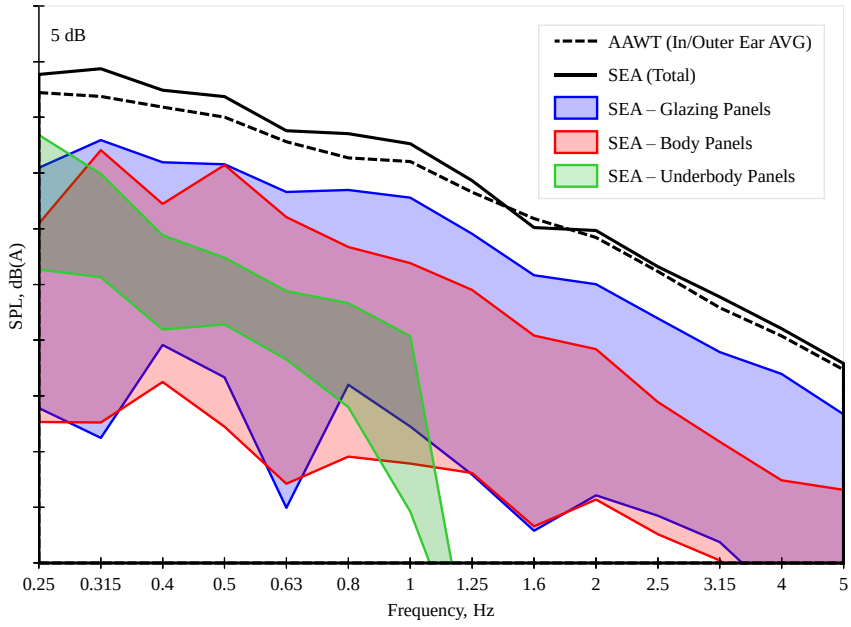

Figure 7: Interior noise at front right head location

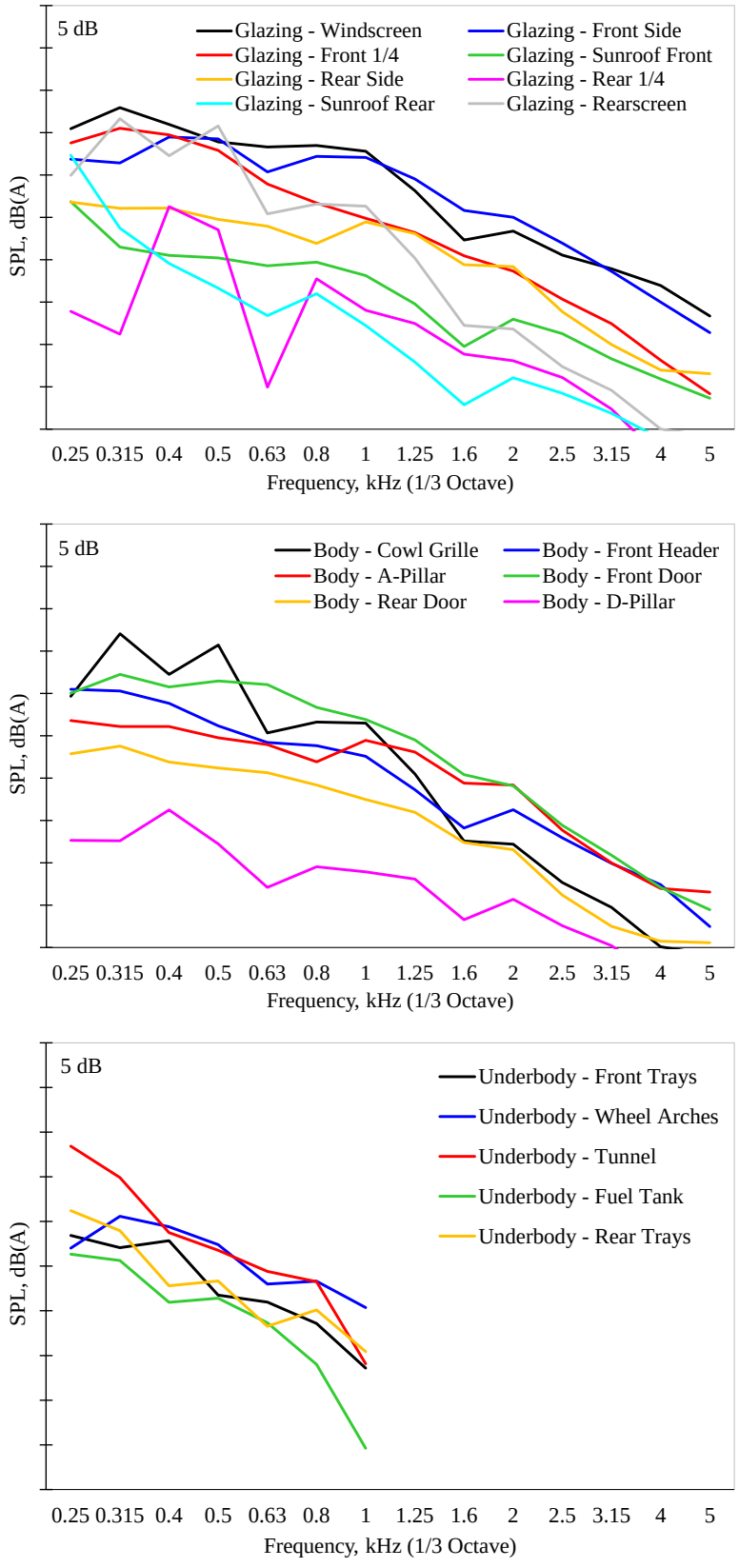

Figure 8: All panels contributions (Top: Glazing panels; Middle: Body panels; Bottom: Underbody panels)

4.2 Glazing & Body Panel Contributions

To investigate the accuracy of the method in predicting the relative contribution of the glazing panels, measurements of glazing blanking taken in the wind tunnel were compared to equivalent estimations from the numerical approach. In the test, A-B insulation material was applied to all panels, and the contribution from un-blanking each panel was measured separately (not cumulative). In the SEA model, the blanking pads were modelled by applying noise control treatment of equivalent specifications to each panel. Figure 9 shows a comparison of the physical test and numerical increments for the most relevant panels to the driver location (Windscreen and Front Side Glass). Contribution from the Windscreen correlates with an offset of 1 dB in lower frequencies, and 2 dB maximum in frequencies above 4kHz. The offset for the Front Side Glass is 2.5 dB maximum in both lower and higher frequencies. The trend between test and numerical data is in good agreement for both panels. Body panel contribution is validated by removing acoustic treatment from specific panels in the test and replicating the change in the SEA model. An example is demonstrated where the insulation from the front door trim is removed and the increment to baseline condition is plotted in Figure 10. The increments match significantly well except from 500 to 800Hz, which is subject for investigation.

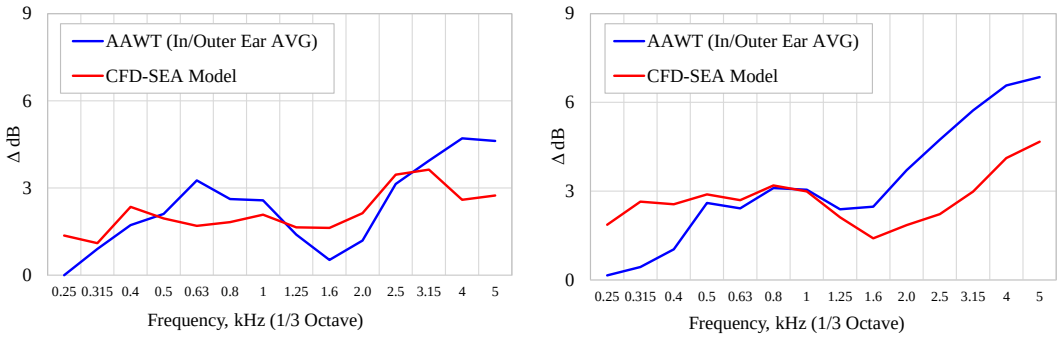

(a) Windscreen (b) Front Side Glass

Figure 9: Glazing blanking contribution analysis (Front Head location)

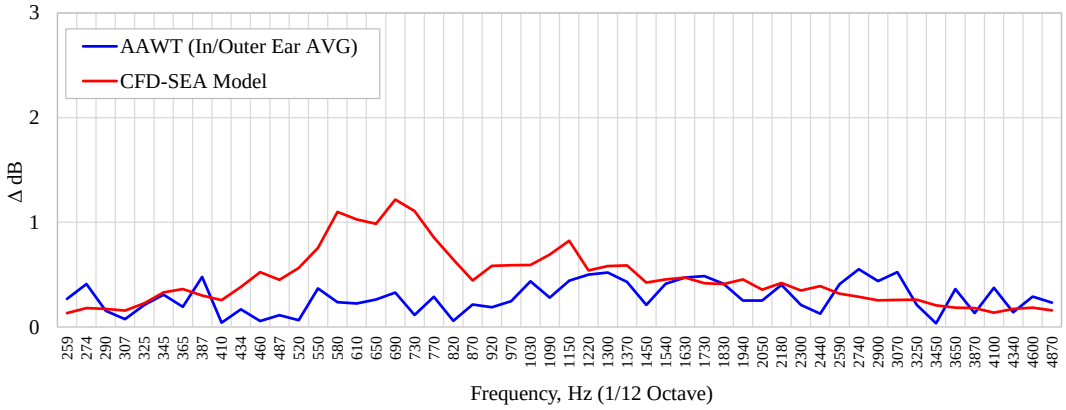

Figure 10: Body panel contribution analysis (Front Head location)

5 Conclusion

Coupling compressible CFD and SEA to support whole-vehicle Aeroacoustics development has been proven as a reliable and realistic methodology. The work undergone to optimize the CFD burden at no accuracy loss has significantly reduced turnaround, and the reuse of Road Noise whole-vehicle SEA models has been proven cost-effective. Correlation offsets are acceptable for whole-vehicle statusing in reference to validated targets, and A-B comparisons of multiple Upper Body and Underbody acoustic specifications have been made possible with the caveat of specific frequency bands under investigation for future projects.

6 Acknowledgements

The authors acknowledge Benjamin West and Holly Daniels for previous developments which ground the present work; as well as Christopher Shaw, Joseph Castle and Boris Fechner from Dassault Systèmes© for constructive partnership.

7 Bibliography

[1] Hartmann, M., Ocker, J., "Wind Noise Caused by the Side-Mirror and A-Pillar of a Generic Vehicle Model", AIAA 2012-2205, 18th AIAA/CEAS Aeroacoustics Conference, 2012, DOI:10.2514/6.2012-2205.

[2] West, B., Daniels, H., Venor, J., and Martin, S., "Development of a Process to Predict Whole Vehicle Aeroacoustic Interior Noise", SAE Technical Paper 2021-01-1047, 2021, DOI:10.4271/2021-01-1047.

[3] Manoha, E., Caruelle, B., "Summary of the LAGOON Solutions from the Benchmark problems for Airframe Noise Computations-III Workshop", AIAA 2015-2846, 21st AIAA/CEAS Aeroacoustics Conference, 2015, DOI:10.2514/6.2015-2846.

[4] Romani, G., Casalino, D., van der Velden, W., "Numerical Analysis of Airfoil Trailing-Edge Noise for Straight and Serrated Edges at Incidence", AIAA JOURNAL Vol. 59, No. 7, July 2021, DOI:10.2514/1.J059457.

[5] Venor, J., Caillet, A., Martin, S., Marz, C. et al., "Using Statistical Energy Analysis to Optimize Sound Package for Realistic Load Cases", SAE Technical Paper 2020-01-1525, 2020, DOI:10.4271/2020-01-1525.

[6] Venor, J., Zopp, A., "Using SEA to Model near Field External Sound Pressure Distributions Based on Automobile Geometry", Vibro-Acoustic Users' Conference, Köln, 2007.